CORA Cork Open Research Archive
Cartlann Taighde Oscailte Chorcaí

Title	A Biopotentiostat-driven read-out system for transfer characteristic-based graphene FET sensing
Authors	Tripathy, Kamalesh;Das, Shrestha;Sica, Marco;Hamidi, Hassan;Iacopino, Daniela;O'Flynn, Brendan;Bhattacharjee, Mitradip
Publication date	2026-10-19
Original Citation	Tripathy, K, Das, S, Sica, M, Hamidi, H, Iacopino, D, O'Flynn, B & Bhattacharjee, M 2026, 'A Biopotentiostat-driven read-out system for transfer characteristic-based graphene FET sensing', IEEE Sensors Journal, pp. 1-8. https://doi.org/10.1109/JSEN.2026.3743185
Type of publication	Article (peer-reviewed)
Link to publisher's version	https://www.scopus.com/pages/publications/105054520895 - 10.1109/JSEN.2026.3743185
Rights	© 2026, IEEE. Personal use of this material is permitted. Permission from IEEE must be obtained for all other uses, in any current or future media, including reprinting/republishing this material for advertising or promotional purposes, creating new collective works, for resale or redistribution to servers or lists, or reuse of any copyrighted component of this work in other works. - https://creativecommons.org/licenses/by/4.0/
Download date	2026-11-07 01:56:27
Item downloaded from	https://hdl.handle.net/10468/19474



University College Cork, Ireland
Coláiste na hOllscoile Corcaigh

This article has been accepted for publication in IEEE Sensors Journal. This is the author's version which has not been fully edited and content may change prior to final publication. Citation information: DOI 10.1109/JSEN.2026.3743185

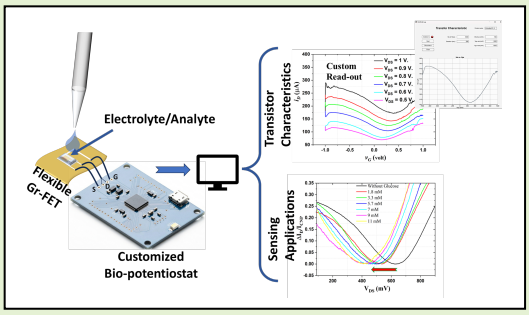
A Biopotentiostat-driven Read-out System for Transfer Characteristic-based Graphene FET Sensing

Kamalesh Tripathy[1], Shrestha Das[1], Marco Sica[2], Hassan Hamidi[2], Daniela Iacopino*[2], Brendan O'Flynn*[2], and Mitradip Bhattacharjee*[1]

[1]i-Lab, EECS Dept., Indian Institute of Science Education and Research Bhopal, Bhopal, India; [2]Tyndall National Institute, University College Cork, Cork, T12 R5CP, Ireland.

*Corresponding Authors: daniela.iacopino@tyndall.ie, brendan.oflynn@tyndall.ie, mitradip@iiserb.ac.in

***Abstract*—Graphene field-effect transistor (Gr-FET) based sensors have emerged as highly promising platforms for biochemical sensing due to graphene's exceptional electrical properties and high sensitivity. Most reported Gr-FET biosensors rely on monitoring the drain current at a fixed gate bias voltage to detect biomarkers. However, such single-point measurements are highly dependent on the chosen operating point and are susceptible to device-to-device variations, drift, and ionic screening in electrolyte environments, which often results in ambiguous sensing responses. A more robust approach is to measure the full transfer characteristics and track the shift in the charge neutrality point (CNP), which directly correlates with variations in surface charge distribution caused by biomolecular interactions. However, acquiring transfer characteristics typically requires bulky and expensive laboratory instrumentation, such as precision source-measure units (e.g., Keithley sourcemeters), and parametric analysers, limiting the practicality of such measurements for portable and real-time sensing applications. In this work, a dedicated electronic readout system based on a bio-potentiostat, referred to as the Custom Readout Module, was developed to measure the transfer characteristics of electrolyte-gated Gr-FET sensors to extract the CNP. System performance was validated against measurements obtained with Keithley 2450 source meters, thereby establishing the platform as a portable solution for extracting transfer characteristics for FET-based biosensing. To demonstrate biosensing capability, the graphene channel was functionalised with glucose oxidase, and glucose was detected in phosphate-buffered saline (PBS) via concentration-dependent CNP shifts. The developed platform provides a reliable solution for transfer-characteristic-based graphene FET biosensing, with potential for portable and real-time sensing applications.**



***Index Terms*— Biopotentiostat, Biosensors, charge neutrality point (CNP), custom electronic readout system, electrolyte-gated graphene FET, transfer characteristics**

I. Introduction

Graphene field-effect transistors (Gr-FETs) have attracted significant attention as next-generation biosensing platforms due to the unique electronic properties of graphene, including high carrier mobility, large surface area, excellent electrical and mechanical properties, intrinsic biocompatibility, and ability to be readily functionalised with receptor biomolecules [1, 2]. These properties allow graphene to exhibit strong electrical responses towards small perturbations in its surface charges, making it highly suitable for label-free biochemical detection. In particular, electrolyte-gated graphene FETs enable direct interaction between the sensing surface and liquid analytes while operating at low voltages. This feature is advantageous for biosensing in physiological environments such as blood, serum, saliva, and sweat. Graphene FETs have been widely investigated as biosensing platforms for various analytes, including proteins, nucleic acids, metabolites, and other biomolecules. In many reported studies, sensing is performed by monitoring the change in drain current at a fixed gate bias after the introduction of the target analyte [1]. Although current-based detection methods are relatively simple to implement, they suffer from several limitations [3-5]. First, the current response depends strongly on the chosen operating bias point along the transfer curve, which may vary from device to device due to fabrication variations, contact resistance, and environmental doping effects. Second, fluctuations in the operating point caused by drift, hysteresis, or ionic screening in electrolyte environments can produce ambiguous responses when measurements are restricted to a single bias point. An alternative and more robust sensing strategy involves monitoring the full transfer characteristics of the Gr-FET and tracking the shift in the charge neutrality point (CNP). In an electrolyte-gated configuration, the graphene channel is in

XXXX-XXXX © XXXX IEEE. Personal use is permitted, but republication/redistribution requires IEEE permission.
See http://www.ieee.org/publications_standards/publications/rights/index.html for more information.
Authorized licensed use limited to: UNIVERSITY COLLEGE CORK. Downloaded on October 21,2026 at 10:15:57 UTC from IEEE Xplore. Restrictions apply.
© 2026 IEEE. All rights reserved, including rights for text and data mining and training of artificial intelligence and similar technologies. Personal use is permitted, but republication/redistribution requires IEEE permission. See https://www.ieee.org/publications/rights/index.html for more information.

This article has been accepted for publication in IEEE Sensors Journal. This is the author's version which has not been fully edited and content may change prior to final publication. Citation information: DOI 10.1109/JSEN.2026.3743185

contact with an ionic solution that resembles the gate dielectric, forming electric double layers (EDLs) at the graphene-electrolyte and gate-electrolyte interfaces [6, 7]. These EDLs provide extremely large capacitance, enabling efficient electrostatic modulation of the graphene channel with small gate voltages. The resulting transfer characteristics of the Gr-FET exhibit the well-known ambipolar behaviour of graphene. The gate voltage at which the channel conductance is minimised is known as the Dirac point, or charge neutrality point (CNP), which marks the transition between electron- and hole-dominated transport. Any modification in the local electrochemical environment at the graphene surface, such as adsorption of charged molecules, pH variations, or biomolecular binding, alters the carrier density in the graphene channel and leads to a measurable shift in the CNP of the transfer characteristics [3, 8]. Since the CNP directly corresponds to the gate voltage at which the net carrier density in graphene is zero, it provides a physically meaningful sensing parameter linked to the electrostatic doping of the graphene channel [9, 10]. The binding of charged biomolecules or enzymatic reactions occurring near the graphene surface introduces additional electrostatic gating, shifting the position of the CNP. Therefore, tracking the CNP offers a more reliable measure of surface charge modulation compared to monitoring drain current at a fixed bias [11]. Moreover, this approach reduces sensitivity to device-to-device variability because the sensing signal is defined by the relative shift of the transfer curve rather than the absolute current magnitude. Despite the advantages of transfer-characteristic-based sensing, its practical implementation requires precise electrical measurement and analysis of the full gate-voltage sweep of the Gr-FET device. Most reported biosensing demonstrations rely on high-precision laboratory instruments such as semiconductor parameter analysers or sourcemeters to obtain the transfer curves, which limits portability and real-time deployment of such sensors [12, 13]. Furthermore, extracting reliable CNP values requires stable bias control, low leakage currents, and convenient visualisation of the transfer characteristics. Consequently, the development of dedicated readout electronics capable of accurately measuring transfer characteristics and tracking CNP shifts is critical for practical Gr-FET biosensing systems.

In this work, a dedicated electronic readout system based on a bio-potentiostat, referred to as the Custom Readout Module, was developed for the electrical characterisation of an electrolyte-gated graphene FET sensor. The system was specifically designed to measure the transfer characteristics of Gr-FET devices. By focusing on the measurement of transfer characteristics rather than single-point current detection, the system enables reliable tracking of electrostatic shifts in the transfer characteristics that are directly linked to biomolecular interactions. The performance of the developed system was experimentally validated by comparing its measurements with those obtained using the standard Keithley 2450 source meters. The results demonstrate that the system can accurately reproduce the transfer characteristics and determine the CNP of electrolyte-gated Gr-FET devices, thereby providing a practical and portable platform for biosensing applications. For validation, glucose sensing was implemented by the Gr-FET biosensing platform through enzymatic glucose detection.

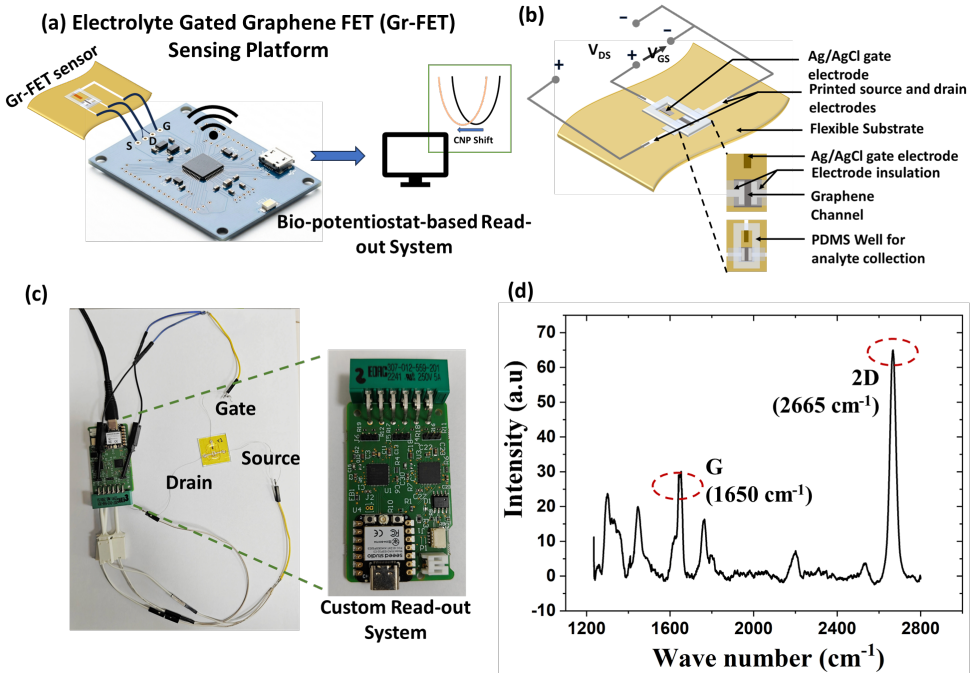


Fig. 1. (a) Schematic illustration of a wireless, miniaturized readout system for acquiring the transfer characteristics of a graphene field-effect transistor (Gr-FET), (b) Design of the flexible Gr-FET device showing source (S), drain (D), and gate (G) electrodes with applied biases, (c) Photograph of the fabricated device connected to the custom portable measurement unit for electrical characterization. (d) Raman spectrum of graphene channel at 632 nm excitation.

Authorized licensed use limited to: UNIVERSITY COLLEGE CORK. Downloaded on October 21,2026 at 10:15:57 UTC from IEEE Xplore. Restrictions apply.
© 2026 IEEE. All rights reserved, including rights for text and data mining and training of artificial intelligence and similar technologies. Personal use is permitted, but republication/redistribution requires IEEE permission. See https://www.ieee.org/publications/rights/index.html for more information.

This article has been accepted for publication in IEEE Sensors Journal. This is the author's version which has not been fully edited and content may change prior to final publication. Citation information: DOI 10.1109/JSEN.2026.3743185

II. Design and Fabrication of Graphene FET Sensor with Bio-Potentiostat System

A. Custom Readout Design

The Custom Readout Module is based on the wireless, reconfigurable electrochemical measurement platform developed at Tyndall National Institute, originally conceived to support a broad range of biochemical sensors [14, 15]. The platform integrates the electrochemical interface with a compact Internet-of-Things microcontroller board (XIAO ESP32C3), built around a 32-bit processor with embedded Wi-Fi and Bluetooth Low Energy connectivity, thereby enabling local device control, data acquisition, wireless communication, onboard memory management, and signal processing. The electrochemical measurement core is implemented using dual AD5940 (16-bit ADC) ultra-low-power analog front-end integrated circuits, which provide programmable potentiostatic control. While the biopotentiostat is primarily intended for conventional electrochemical sensing with working, counter, and reference electrodes, the readout module was further adapted to interface with a three-terminal graphene field-effect transistor (Gr-FET) for transfer characteristic measurements. In this operating mode, one analog front end maintains a constant drain-source voltage (V_{DS}), while the second sweeps the gate-source voltage (V_{GS}); the resulting drain current (I_D) is then recorded, thereby enabling electrical characterisation of the Gr-FET. The schematic of the Gr-FET integration with the bio-potentiostat and its circuit interfacing is showcased in Fig. 1 (a) and (c). The firmware running on the microcontroller controls the measurement operations of the device. It sets the measurement protocols, applies the required bias voltage to the electrodes, and collects current measurement data from the sensor. Signal conditioning and noise reduction are performed using the integrated digital filtering of the AD5940 prior to data transmission. Wireless communication enables real-time data streaming to external interfaces such as MATLAB-based or mobile applications for visualisation, configuration of sensor calibration tests, and export of measurement data. A MATLAB-based user interface was developed for the real-time transfer characteristics measurement and user control.

B. Gr-FET Fabrication

Monolayer graphene on copper foil (Gr/Cu), ammonium persulphate, and $FeCl_3$, sodium alcohol ether sulphate (AES) were procured from Sigma Aldrich to fabricate the Gr-FET. The electrodes were printed using conductive silver ink (Voltera) with the help of Voltera V-one PCB printer, and polydimethylsiloxane (PDMS: Sylgard-184, Dow Chemicals) was used for insulation. Kapton tape (OTOVON), a 25 µm-thick thermal lamination film (SAGBAN), were used for the substrate and graphene transfer. For surface functionalization

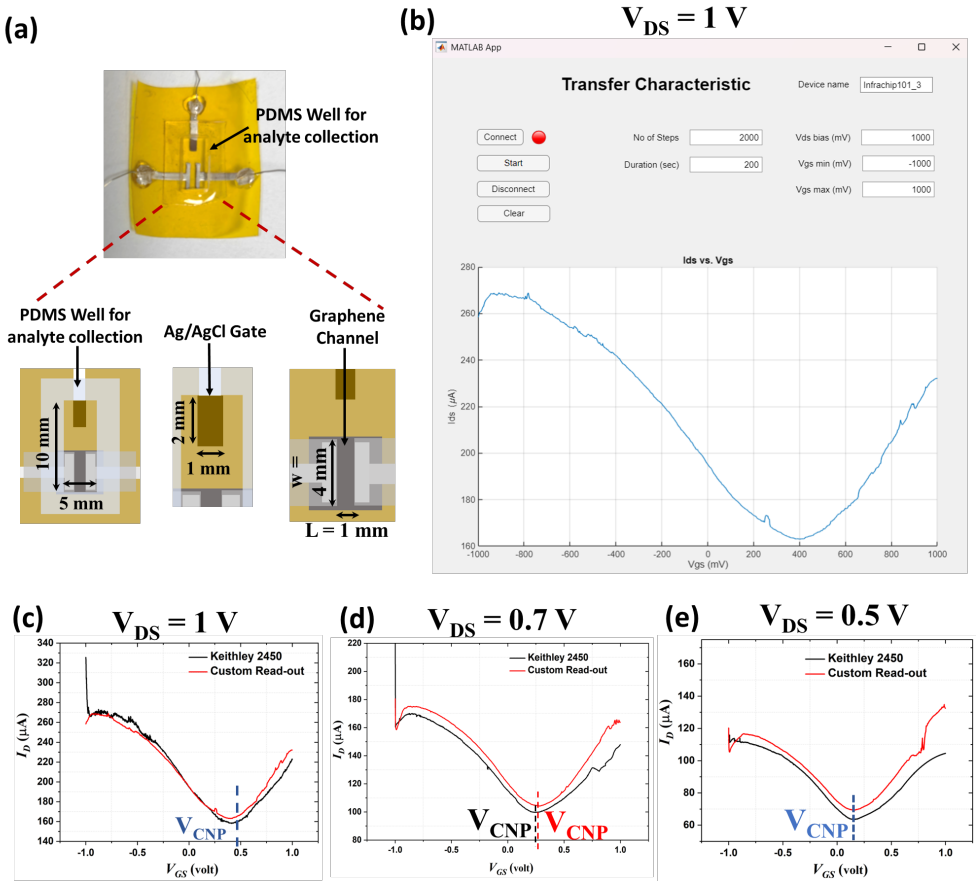


Fig. 2. (a) Fabricated Gr-FET with its geometrical dimensions (b) Screenshots of the user-interface window showing transfer characteristics (I_D vs. V_{GS}) of the Gr-FET device with drain voltage V_{DS} = 1 V measured using the Custom Readout Module. (c-e) Comparison of transfer characteristics obtained using a Keithley 2450 source meter (black) and the Custom Readout Module (red), with different drain voltages (V_{DS} = 1 V, 0.7 V, and 0.5 V.).

Authorized licensed use limited to: UNIVERSITY COLLEGE CORK. Downloaded on October 21,2026 at 10:15:57 UTC from IEEE Xplore. Restrictions apply.
© 2026 IEEE. All rights reserved, including rights for text and data mining and training of artificial intelligence and similar technologies. Personal use is permitted, but republication/redistribution requires IEEE permission. See https://www.ieee.org/publications/rights/index.html for more information.

This article has been accepted for publication in IEEE Sensors Journal. This is the author's version which has not been fully edited and
content may change prior to final publication. Citation information: DOI 10.1109/JSEN.2026.3743185

of graphene and subsequent sensing experiments, 1-pyrenebutyric acid N-hydroxysuccinimide ester (PASE), N,N-dimethylformamide (DMF), phosphate-buffered saline (PBS), D-(+)-glucose, and glucose oxidase were procured from Sigma Aldrich.

The fabrication of Gr-FET begins with graphene transfer on a flexible substrate comprised of a lamination layer on Kapton tape via the heat transfer method [16]. The CVD-grown graphene on copper foil (Gr/Cu) was laminated on the lamination layer at 90 °C on a hot plate. The copper was etched away by dipping it into 5 % ammonium persulfate solution for 4 hours. Three electrodes were printed with the help of the Voltera V-One PCB printer using silver ink to have source, drain and gate as shown in Fig. 1 (b). PDMS layers were brushed on the source and drain electrodes for insulation against the analyte. The AgCl was grown on the surface of the Ag gate electrode to have Ag/AgCl gate electrode for stable FET characteristics. A plating solution (0.25 M $FeCl_3$, 0.35% sodium alcohol ether sulphate (AES) in DI water) was drop-cast on the Ag gate electrode with a treatment time of 1 hr for stable growth of AgCl. After the AgCl growth, the electrodes were rinsed with DI water, and the transfer characteristics were measured. For the Ag/AgCl gate protection, 0.2% nafion in ethanol solution was drop-cast on the gate electrode, and let it dry at room temperature. Then it was heated at 70 °C for 30 min. The graphene channel was further functionalised by 5 mM PASE (1-Pyrenebutyric acid N-hydroxysuccinimide ester) in DMSO for 2 hours. A 10 mg mL^{-1} glucose oxidase solution in PBS was used for incubate the graphene channel to immobilise the glucose oxidase (GOx) enzyme on the graphene surface, and the device was subsequently stored at 8 °C for 14 hr to allow stable enzyme attachment. Phosphate buffer saline (PBS) was used as the electrolyte in all the experiments and acts as the electrolyte gate in the Gr-FET structure. The sensor was calibrated with glucose solutions of different concentrations in PBS with the help of the Custom Readout Module.

III. Results and Discussion

After transferring graphene onto the substrate, Raman spectroscopy was performed to characterise the sample. The graphene unit cell contains two carbon atoms and has 6 phonon dispersion bands, each atom having 3 independent modes. Among these, 3 are optical, and the other 3 are acoustic phonon branches. Among these modes, the ones sensitive to Raman spectroscopy produce two distinctive peaks: the G band and the 2D band. The Raman spectra of the transferred graphene on the substrate were obtained with a laser source with a wavelength

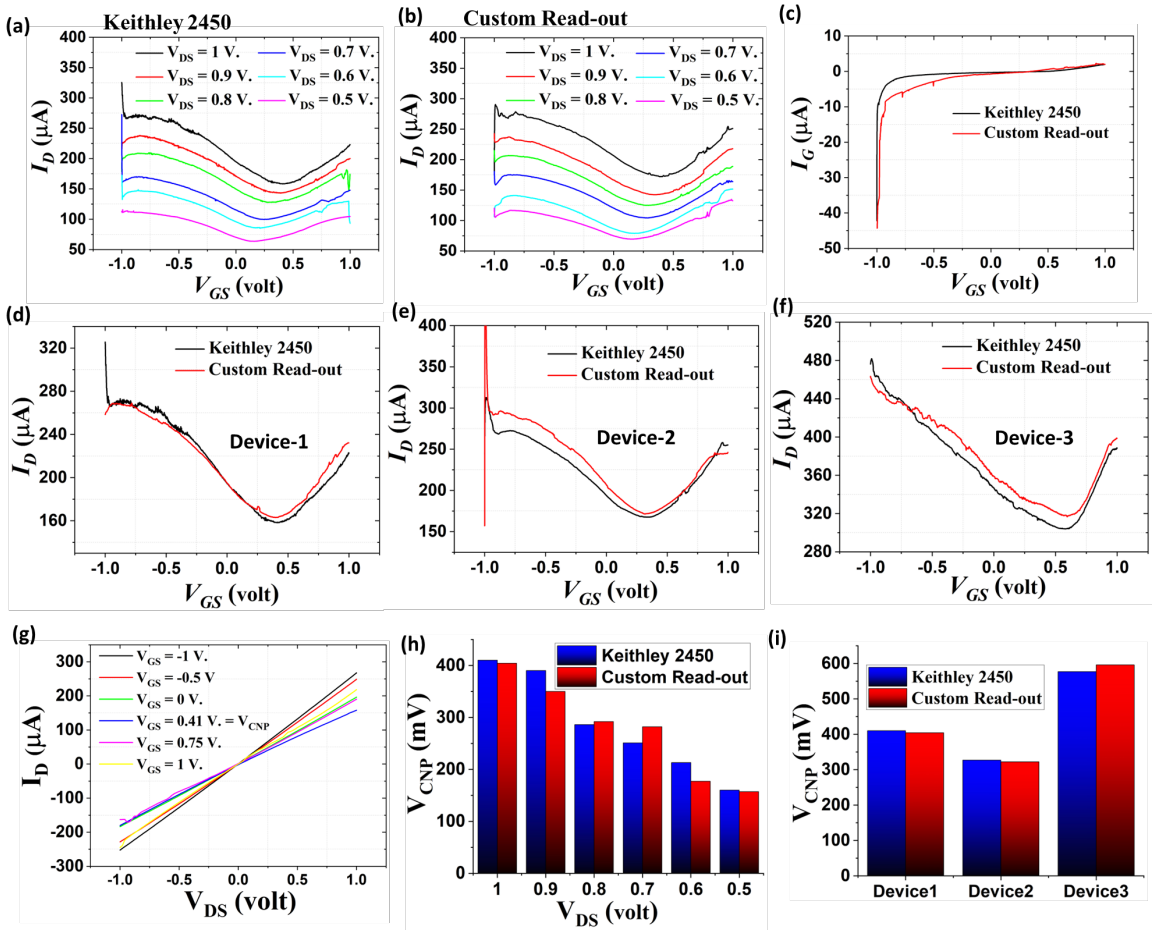


Fig. 3. (a) Transfer characteristics of a graphene FET measured at different drain biases (V_{DS}) using a Keithley 2450 source meters, (b) corresponding transfer characteristics measured using the Custom Readout Module under identical bias conditions, showing comparable trends, (c) comparison of gate leakage current trends for Ketley 2450 and Custom Readout Module (d–f) Direct comparison of transfer characteristics for three different devices (Device-1, Device-2, and Device-3), measured using the Keithley 2450 source meter (black) and the Custom Readout Module (red), (g) output characteristics of Device-1 with different drain to source voltages V_{DS}.

Authorized licensed use limited to: UNIVERSITY COLLEGE CORK. Downloaded on October 21,2026 at 10:15:57 UTC from IEEE Xplore. Restrictions apply.
© 2026 IEEE. All rights reserved, including rights for text and data mining and training of artificial intelligence and similar technologies. Personal use is permitted,
but republication/redistribution requires IEEE permission. See https://www.ieee.org/publications/rights/index.html for more information.

This article has been accepted for publication in IEEE Sensors Journal. This is the author's version which has not been fully edited and content may change prior to final publication. Citation information: DOI 10.1109/JSEN.2026.3743185

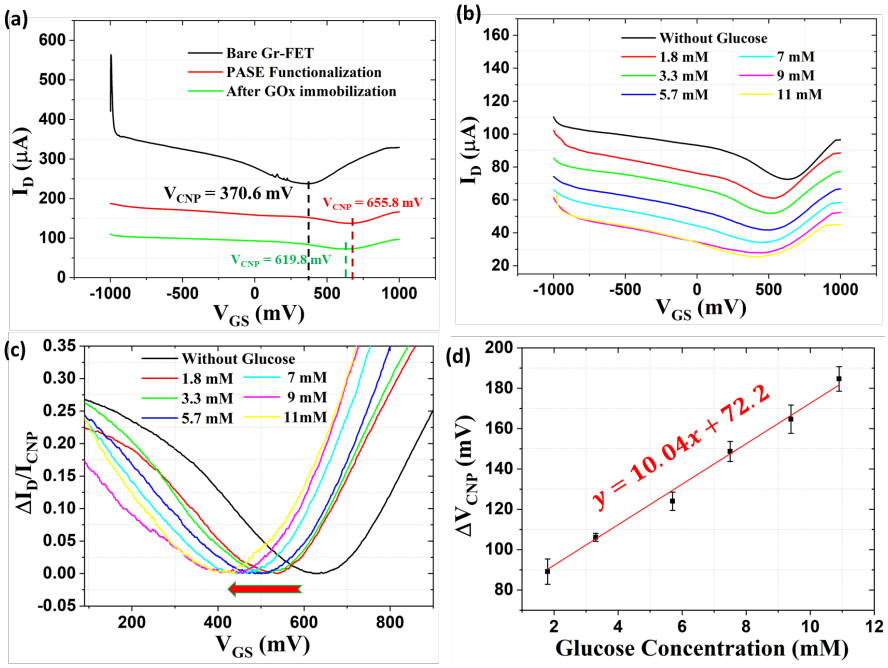


Fig. 4. (a) Transfer characteristics of the graphene FET at different functionalization stages: bare device, after PASE functionalization, and after glucose oxidase (GOx) immobilisation, (b) transfer characteristics of the functionalized Gr-FET device at varying glucose concentrations, (c) transfer characteristics with the normalised current response ($\Delta I_D/I_{CNP}$ vs V_{GS}) to show the shift in V_{CNP} with varying glucose concentration, (d) calibration curve showing the shift in charge neutrality point (ΔV_{CNP})as a function of glucose concentration, exhibiting a linear response.

of 632 nm, as shown in Fig. 1 (d). The G and 2D peaks of graphene are shown in the graph at 1650 cm^{-1} and 2665 cm^{-1}, respectively. For electrical characterisation of Gr-FETs, phosphate-buffered saline (PBS) was used as the electrolyte, and transfer characteristics were acquired using the Custom Readout Module and validated with Keithley 2450 source meters. Fig. 2 (a) provides the detailed physical dimensions of the Gr-FET, i.e., graphene channel dimensions (w and L) defined by printed source and drain silver electrodes, and the dimensions of the PDMS well (Area: 10 mm × 5 mm) for analyte collection. The width-to-length aspect ratio (w/L) of the graphene channel is 4:1. A volume of 100 µl of analyte was used through all of the experiments in the PDMS well. The transfer characteristics of Gr-FET exhibit ambipolar behaviour, and the gate voltage corresponding to the minimum drain current I_D is referred to as the Dirac voltage or charge neutrality point (V_{CNP}), as illustrated in later transfer characteristics measurements in Fig. 2. The working principle of Gr-FET-based sensors is described in section S1 in the Supporting Information document. Fig. 2 (a)-(c) shows the transfer characteristics measured by the Custom Readout Module using the developed user interface at different drain-to-source voltages (V_{DS}) spanning from 1 V to 0.5 V. Further, these measurements of the transfer characteristics of the Gr-FET by the Custom Readout Module were validated against the standard measurements obtained using the Keithley source meter 2450. Here, two source meters were used in master-slave connection to obtain the transfer characteristics of the Gr-FETs. Fig. 2 (d)-(f) shows the comparative transfer characteristics of the Gr-FET with the source meters and the custom read-out module. Fig. 3 (a) and (b) show the transfer characteristics obtained at different V_{DS} i.e., $V_{DS} = 1\,V, 0.9\,V, 0.8\,V, 0.7\,V, 0.6\,V$ and $0.5\,V$ with the Keithley 2450 source meter (black) and the Custom Readout Module (red). It can be observed that the transfer characteristics measured by the Custom Readout Module closely follow the source meter measurement. Moreover, the transfer characteristics show V_{CNP} shifts leftwards with decreasing values of V_{DS}. In graphene field-effect transistors (FETs), the charge neutrality point (CNP), represents the gate voltage where electron and hole densities balance out, yielding minimum conductivity. When the magnitude of V_{DS} is large in a long-channel device, the drain injects additional electrons into the graphene channel. To reach charge neutrality, the gate must apply a higher compensating voltage, shifting V_{CNP} towards more positive voltages. Similarly, when V_{DS} decreases, drain-induced charge modulation weakens and, as a consequence, V_{CNP} shifts leftward. The shifts in transfer characteristics with varying V_{DS} in both cases were also found to be similar, as shown in Fig. 3 (a) and (b). Further, the measurement accuracy of the Custom Readout Module was tested by measuring multiple devices for their electrical characterisation, and the transfer characteristics of 3 different Gr-FET devices are presented in Fig. 3 (d-f). The gate leakage current (I_G) for the Custom Readout Module was measured by a Keithley digital multimeter (DMM 6500) connected in series at the gate terminal and presented in Fig. 3 (c). The measurement of I_G by the Custom Readout Module closely follows the measurement by the Keithley sourcemeters, except at the initial gate voltages (V_{GS}), where a transient increase in the gate current is observed during the switching-on process. Fig. 3 (g) shows the output characteristics ($I_D \sim V_{DS}$) with different gate-to-source voltages (V_{GS} = -1 V, -0.5 V, -0.41 V, 0.75 V, and 1 V). The device exhibits a linear, ohmic $I_D \sim V_{DS}$ relationship through the origin across the full V_{DS} range at every gate bias (V_{GS}), confirming operation in the linear/triode regime. Furthermore, the slope (channel conductance) varies

Authorized licensed use limited to: UNIVERSITY COLLEGE CORK. Downloaded on October 21,2026 at 10:15:57 UTC from IEEE Xplore. Restrictions apply.
© 2026 IEEE. All rights reserved, including rights for text and data mining and training of artificial intelligence and similar technologies. Personal use is permitted, but republication/redistribution requires IEEE permission. See https://www.ieee.org/publications/rights/index.html for more information.

This article has been accepted for publication in IEEE Sensors Journal. This is the author's version which has not been fully edited and content may change prior to final publication. Citation information: DOI 10.1109/JSEN.2026.3743185

systematically with ($V_{GS} - V_{CNP}$) as predicted by the model, i.e., the curve at $V_{GS} = V_{CNP}$ shows the minimum slope, while the curve furthest from the Dirac point shows the steepest slope, with the remaining output curves ordered consistently with their distance from V_{CNP}. Fig. 3(h) directly compares the extracted charge neutrality points V_{CNP} between the Keithley 2450 SMU and the custom readout across applied drain-to-source V_{DS} voltages ranging from 0.5 V to 1 V, demonstrating that both instruments capture the systematic leftward shift in V_{CNP} as V_{DS} decreases. Further, Fig. 3(i) shows the extracted V_{CNP} values across three distinct devices at V_{DS} = 1 V, i.e., the operating point for the sensors. This confirms consistent device-to-device measurements between the two measurement platforms. The differences between the V_{CNP} for these 3 devices are 1.4 %, 1.5%, and 3 % of the SMU measurement values, respectively, validating the measurement by the designed read-out circuit.

Further, the Gr-FET platform was functionalised with glucose oxidase to detect glucose in PBS to demonstrate its biosensing capability. The GOx is immobilised using PASE linker molecule layer on the graphene channel. Fig. 4 (a) shows changes in its transfer characteristics and shifts in the V_{CNP} after PASE functionalization and Gox immobilisation. The observed shifts in V_{CNP} are governed by interfacial charge-transfer and electrostatic gating effects at the graphene surface. The non-covalent bonding of PASE via π-π stacking with graphene introduces strongly electron-withdrawing succinimidyl ester groups, which withdraw electron density from the graphene lattice. This causes p-type doping behaviour shifting V_{CNP} positively from 370.6 mV to 655.8 mV. Further, covalent bonding of glucose oxidase (GOx) via nucleophilic substitution between its primary amine groups (-NH_2) and the active ester group of PASE leads to a slight negative relaxation to 619.8 mV, which arises from partial electrostatic charge neutralisation and local dielectric screening. After the graphene channel was modified by the Gox, Different concentrations of D-glucose in PBS, ranging from 1.8 mM to 11 mM were introduced to the sensor, and the transfer characteristics were obtained with the Custom Readout Module. To evaluate the hysteresis effect on CNP, forward and reverse gate-voltage sweeps between −1 V and +1 V were compared. This shows a difference of approximately 26 mV in CNP, as shown in Fig. S1 in the Supporting Information document. This indicates a relatively small but measurable hysteresis-related shift. Additionally, time-dependent measurements following glucose exposure showed that the transfer characteristics obtained after 5 min. and 10 minutes were in close agreement, suggesting that the electrical response approached a stable condition within approximately 5 minutes, and the same is shown in Fig. S2 in the Supporting Information document. For the glucose-sensing measurements, the same gate-voltage sweep protocol and readout configuration were maintained across all concentrations. After each measurement, the sensing region was washed with PBS before introducing the subsequent glucose concentration. All measurements were taken after 5 min. from the instant the analyte was dropped into the PDMS well. The sensing mechanism of glucose detection is explained in section S2 of the Supporting Information document. Here, to show the shift in CNP, the drain current is normalised as $\frac{\Delta I_D}{I_{CNP}} = \frac{I_D - I_{CNP}}{I_{CNP}}$ and plotted against V_{GS} in Fig. 4 (c). The shift in V_{CNP} showed a monotonic dependence over the investigated concentration range (1.8–11 mM). The calibration curve in Fig. 4 (d) shows the shift in CNP, i.e., ΔV_{CNP} against different glucose concentrations. The calibration curve exhibits good linearity with COD (R^2) = 0.992, and the slope of the calibration curve shows a sensitivity of 10 mV/mM. The sensor exhibits a larger shift in the CNP at a concentration of 1.8 mM with respect to the solution with no glucose, as shown in Fig. 4(c). This non-linearity at low concentration can be explained by Michaelis-Menten enzyme kinetics [17] and interfacial electrostatic equilibrium. Immobilised glucose oxidase (GOx) catalyses the oxidation of glucose, producing byproducts (H_2O_2 and gluconic acid) that alter the local Debye screening layer and donate electrons to the graphene channel. At low glucose concentrations, the enzymatic reaction rate increases non-linearly with concentration, causing a sharp initial change in local interfacial charge before settling into a steady, diffusion-moderated response across intermediate concentrations. Here, Table-1[18-22] provides a comparative overview of the proposed system and the FET read-out platforms reported in the

Table 1: Comparison of Portable and Integrated FET Readout and Characterisation Systems

Sensing Platform	*DAC / ADC resolution*	*Voltage sweep*	*Sampling Rate*	*Wireless / Connectivity*	*Size*	*Ref*
GFET array for SARS-CoV-2 detection	ADC: 16-bit, 8-channel;	V_{GS}: 0–0.9 V	30 kSPS ADC; 1 Mbps USB transfer	No	NR	[22]
EGFET array ion sensing	DAC: dual 12-bit; ADC: 12-bit	V_{GS}: −0.6 to +0.9 V	NR	No	cell-phone size	[21]
CMOS-integrated GFET biosensor array	NR	NR	NR	No	Wafer scale	[23]
Commercial Graphenea GFET-S20	ADC: 31-bit, ~22-bit effective	V_{GS}: 0 to +1.5 V	4.096 ms or 160 ms sampling times	BLE	35 × 40 mm²	[4]
Low-cost SMU for FET sensor	DAC: 12-bit; ADC: 12-bit	±10 V / ±1.25 V	NR	No	NR	[5]
Biopotentiostat / Full Transfer Curve (ID – VGS sweep)	**16-bit ADC**	**±1.0 V**	**100 Hz (2000 pts / 200 s)**	**Yes (BLE / USB)**	**~ (67 × 33 mm²)**	**This Work**

*NR: Not Reported

Authorized licensed use limited to: UNIVERSITY COLLEGE CORK. Downloaded on October 21,2026 at 10:15:57 UTC from IEEE Xplore. Restrictions apply.
© 2026 IEEE. All rights reserved, including rights for text and data mining and training of artificial intelligence and similar technologies. Personal use is permitted, but republication/redistribution requires IEEE permission. See https://www.ieee.org/publications/rights/index.html for more information.

This article has been accepted for publication in IEEE Sensors Journal. This is the author's version which has not been fully edited and
content may change prior to final publication. Citation information: DOI 10.1109/JSEN.2026.3743185

literature. The comparison illustrates the diversity of existing approaches and presents the contribution of the proposed system in extracting complete transfer characteristics of electrolyte-gated Gr-FETs using a reconfigurable bio-potentiostat architecture.

IV. Conclusion

In this work, a dedicated readout system for electrolyte-gated Gr-FET sensors was successfully developed and experimentally validated. The miniaturised bio-potentiostat-based read-out system, referred to as the "Custom Readout Module", demonstrated reliable measurement of the transfer characteristics to extract the charge neutrality point across multiple devices, with close agreement to standard sourcemeter measurements. The observed leftward shift of the CNP with decreasing drain-source voltage was consistently captured, confirming the system's sensitivity to drain-induced electrostatic effects. Furthermore, the graphene channel was successfully functionalised with glucose oxidase to detect glucose in laboratory settings to demonstrate the biosensing capability of the stand-alone sensor system. The Custom Readout Module can also be used to measure transfer characteristics of Bio-FETs and associated sensing platforms, as an alternative to bulky laboratory instrumentation like sourcemeters and parametric analysers for specific applications. The overall results establish the Custom Readout Module as a practical and effective solution for Gr-FET sensor characterisation and future biosensing applications.

Acknowledgment

The authors would like to acknowledge the support provided by the INFRACHIP (EU Horizon Europe Grant No. 101131822) for facilitating this research. Aspects of this work have been supported by the financial support of Taighde Éireann – Research Ireland on behalf of the Government of Ireland under Grant 12/RC/ 2289-P2-INSIGHT, 13/RC/2077-2CONNECT and 21/RC/10303_P2-VISTAMILK 2, which are co-funded by the European Regional Development Fund (ERDF) under Ireland's European Structural and Investment Funds Programme. The authors also express their sincere gratitude to the Central Instrumentation Facility (CIF) at IISER Bhopal for access to characterisation facilities. We further thank the Department of Electrical Engineering and Computer Science (EECS), IISER Bhopal, and Tyndall National Institute for providing the necessary infrastructure and equipment to carry out this work.

For the purpose of Open Access, the author has applied a CC BY public copyright license to any Author Accepted Manuscript version arising from this submission.

References

[1] C. D. Pham, Q. T. Trinh, J. Zhang, N. T. Nguyen, and T. K. Nguyen, "Pushing Biomolecule Detection Limit With Graphene Field-effect Transistor Biosensors," *Advanced Electronic Materials,* vol. 11, no. 19, p. e00368, 2025.

[2] Y.-T. Wang *et al.*, "A comprehensive review of graphene-based biosensors: Fabrication, applications, characterization and future perspectives—A review," *APL bioengineering,* vol. 9, no. 3, 2025.

[3] C. Reiner-Rozman, M. Larisika, C. Nowak, and W. Knoll, "Graphene-based liquid-gated field effect transistor for biosensing: Theory and experiments," *Biosensors and Bioelectronics,* vol. 70, pp. 21-27, 2015.

[4] T. Ono, S. Okuda, S. Ushiba, Y. Kanai, and K. Matsumoto, "Challenges for field-effect-transistor-based graphene biosensors," *Materials,* vol. 17, no. 2, p. 333, 2024.

[5] M. Pawar, P. Yadav, G. HN, T. P. Sai, S. Gandhi, and A. Ghosh, "Challenges in Graphene-Based Biosensing: Exploring Critical Limitations and Strategies," *ACS sensors,* vol. 11, no. 1, pp. 86-94, 2025.

[6] C. D. Pham, Q. T. Trinh, J. Zhang, N.-T. Nguyen, and T.-K. Nguyen, "Pushing Biomolecule Detection Limit With Graphene Field-effect Transistor Biosensors," *Advanced Electronic Materials,* vol. 11, no. 19, p. e00368, 2025, Art no. e00368,

[7] S. Ghosh, N. I. Khan, J. G. Tsavalas, and E. Song, "Selective Detection of Lysozyme Biomarker Utilizing Large Area Chemical Vapor Deposition-Grown Graphene-Based Field-Effect Transistor," (in English), *Frontiers in Bioengineering and Biotechnology,* Original Research vol. Volume 6 - 2018, 2018-March-22 2018, doi: 10.3389/fbioe.2018.00029.

[8] M. Sun *et al.*, "Flexible graphene field-effect transistors and their application in flexible biomedical sensing," *Nano-Micro Letters,* vol. 17, no. 1, p. 34, 2025.

[9] N. Norhakim, T. Gunasilan, Z. R. Kesuma, H. F. Hawari, and Z. A. Burhanudin, "Elucidating the time-dependent charge neutrality point modulation of polymer-coated graphene field-effect transistors in an ambient environment," *Nanotechnology,* vol. 35, no. 50, p. 505201, 2024.

[10] K. Kikuchi, Y. Yamazaki, K. Kanekura, and Y. Hayamizu, "Graphene Biosensor Differentiating Sensitive Interactions between Ribonucleic Acid and Dipeptide Repeats in Liquid–Liquid Phase Separation," *ACS Applied Materials & Interfaces,* vol. 17, no. 8, pp. 12765-12771, 2025.

[11] S. Ushiba *et al.*, "Biosensing with surface-charge-modulated graphene field-effect transistors beyond nonlinear electrolytic screening," *ACS omega,* vol. 8, no. 51, pp. 49270-49277, 2023.

[12] A. Béraud, M. Sauvage, C. M. Bazán, M. Tie, A. Bencherif, and D. Bouilly, "Graphene field-effect transistors as bioanalytical sensors: Design, operation and performance," *Analyst,* vol. 146, no. 2, pp. 403-428, 2021.

[13] M. T. Hwang *et al.*, "Ultrasensitive detection of nucleic acids using deformed graphene channel field effect biosensors," *Nature communications,* vol. 11, no. 1, p. 1543, 2020.

[14] M. Sica, M. Rasel, B. O'Flynn, H. Hamidi, and D. Iacopino, "A Novel Wireless, Wearable Potentiostat for On-Body Electrochemical Sensing," in *2025 IEEE SENSORS*, 2025: IEEE, pp. 1-4.

[15] L. Khokhlova, H. Hamidi, M. Sica, D. Iacopino, and B. O'Flynn, "Wireless, reconfigurable electrochemical measurement platform for wearable applications," in *2025 IEEE Applied Sensing Conference (APSCON)*, 2025: IEEE, pp. 351-354.

[16] K. Tripathy and M. Bhattacharjee, "High-Performance Flexible and Printed Graphene-Field Effect Biosensor for Ferritin Detection," *Advanced Materials Technologies,* vol. 10, no. 7, p. 2401292, 2025.

[17] X. Zhang, J. Xin, and R. Jin, "Electrochemical glucose sensing using an electrochemically reduced graphene oxide/poly-L-lysine composite electrode modified with glucose oxidase," *International Journal of Electrochemical Science,* p. 101357, 2026.

[18] L. Xu *et al.*, "On-chip integrated graphene aptasensor with portable readout for fast and label-free COVID-19 detection in virus transport medium," *Sensors & diagnostics,* vol. 1, no. 4, pp. 719-730, 2022.

[19] M. Xue *et al.*, "Integrated biosensor platform based on graphene transistor arrays for real-time high-accuracy ion sensing," *Nature Communications,* vol. 13, no. 1, p. 5064, 2022/08/27 2022, doi: 10.1038/s41467-022-32749-4.

[20] M. Soikkeli *et al.*, "Wafer-scale graphene field-effect transistor biosensor arrays with monolithic CMOS readout," *ACS Applied Electronic Materials,* vol. 5, no. 9, pp. 4925-4932, 2023.

[21] G. Biagetti, P. Crippa, M. Alessandrini, and D. Di Marino, "Portable high-accuracy wireless acquisition system for graphene-based sensors," *IEEE Sensors Journal,* vol. 23, no. 15, pp. 17011-17024, 2023.

[22] A. M. Galanti and M. A. Haidekker, "Low-cost source measure unit (SMU) to characterize sensors built on graphene-channel field-effect transistors," *Sensors,* vol. 24, no. 12, p. 3841, 2024.

Authorized licensed use limited to: UNIVERSITY COLLEGE CORK. Downloaded on October 21,2026 at 10:15:57 UTC from IEEE Xplore. Restrictions apply.
© 2026 IEEE. All rights reserved, including rights for text and data mining and training of artificial intelligence and similar technologies. Personal use is permitted,
but republication/redistribution requires IEEE permission. See https://www.ieee.org/publications/rights/index.html for more information.

This article has been accepted for publication in IEEE Sensors Journal. This is the author's version which has not been fully edited and content may change prior to final publication. Citation information: DOI 10.1109/JSEN.2026.3743185



Kamalesh Tripathy received the Ph.D. degree from the Indian Institute of Science Education and Research Bhopal, India. He is currently working as a Research Intern Fellow at Intisen Technology Pvt. Ltd., IICE, IISER Bhopal. He has authored/co-authored more than 20 research articles in reputed journals/conferences, and filed 3 patents. His research interests include flexible/printed and wearable electronics, biosensors, bioelectronics, electronic sensors, and systems.



Shrestha Das received the M.Sc. degree in Electronics from West Bengal State University, India in the year 2022.She has qualified National Eligibility Test (UGC NET), India in Assistant Professorship category. She is currently pursuing Ph.D. degree at the i-Lab research group, Department of Electrical Engineering and Computer Science, Indian Institute of Science Education and Research Bhopal, India. Her research interests include biosensors, electronic sensors, wearable devices and flexible electronics. She has published conference paper in reputed conference and is working for ongoing research projects.



Marco Sika earned his BSc and MSc in Biomedical Engineering at the University Federico II, Napoli, Italy and Polytechnic of Torino, Italy, respectively. In 2016, he joined Tyndall National Institute, Cork, Ireland. Marco's research work is focused on hardware and firmware design, digital signal processing, and data analytics.



Dr. Hassan Hamidi received the Ph.D. degree in Analytical Chemistry from the Institute for Advanced Studies in Basic Sciences, Zanjan, Iran in 2010. He was awarded the prestigious Marie Skłodowska-Curie Individual Fellowship in 2020. He joined the Nanotechnology Group at Tyndall National Institute, University College Cork, Cork, Ireland, as an Experienced Researcher in 2021. His research interests include electrochemical sensors and biosensors, analytical chemistry, sustainable platforms and technologies, biomedical diagnostics, and advanced electrochemical detection systems.



Dr Daniela Iacopino is a senior researcher and leader of the "Integrated Nanomaterials" team at the Tyndall National Institute. Daniela has expertise in fabrication of functional nanoscale materials and their application in health, environmental monitoring and energy. Within her research team, special focus is devoted to the development of green materials and fabrication techniques for fabrication of sustainable wearable sensing and energy electronics. Daniela has participated (both as coordinator and partner) to 15 EU projects, spanning from FP7 to H2024 EU frameworks. She is also the recipient of several national grants. Daniela is a Funded Investigator in the Research Ireland (RI) national centres of excellence CONNECT and VistaMilk. Daniela has published over 100 scientific manuscripts, graduated eight PhD students and supervised/mentored over 20 master students and three staff researchers.



Dr Brendan O'Flynn received his BE 1993, in 1995 received his M Eng Sc degree and in 2017 was awarded his PHD from University College Cork. Dr O'Flynn is a senior head of group for the Wireless Sensor Network activities at Tyndall and also leads the Human Centric (Smart) systems research activity at Tyndall. The WSN group is employing a system level design methodology focusing on the development of the embedded software and energy aware system intelligence, the necessary deployment tools to get systems into the field and ensure long lifetime deployments of complex sensing platforms.
Brendan's research interests' lie in the areas of sensor system integration, low power embedded system design and development (hardware and software), algorithm development for embedded system data fusion, system miniaturization, RF system design and optimization and system deployment. Dr O'Flynn is an adjunct professor at the Indian Institute of Technology in Hyderabad (IITH) India at the department of Mechanical and Aerospace Engineering.



Dr. Mitradip Bhattacharjee (Senior Member, IEEE) is an Associate Professor with the Electrical Engineering and Computer Science Department, Indian Institute of Science Education and Research (IISER) Bhopal, India, where he is leading the i-Lab Research Group. His research interests include electronic sensors and systems, biomedical engineering, bioelectronics, implantable and ingestible electronics, flexible/printed and wearable electronics, wireless systems, IoT, micro/nanoelectronics, softrobotics, m-Healthcare, AI/ML in sensing, and reconfigurable sensing antennas. He has authored more than 100 research articles in reputed journals/conferences and filed more than 28 national/international patents. He has also authored several book chapters/books to date. He is the recipient of several awards and honours, such as the INAE Young Engineer Award in 2025,INAE Young Associate 2025, Young Professional Award by IEEE Sensors Council, USA in 2025, the Visvesvaraya YFR Fellowship by MeitY, Govt. of India in 2025, the Marie-Curie Seal of Excellence Award by the European Commission in 2019, the Nanochallenge Award by PSG in 2018, the Gandhiyan Young Technological Innovation Award at Rashtrapati Bhavan in 2016, among others. He served as the chair of the IEEE Sensors Council Young Professionals, USA in 2022. He is serving as a guest editor and associate editor in various journals and magazines such as IEEE IoT Journal, IEEE Sensors Letters, IEEE Sensors Alert, IEEE JFLEX, npj Flexible Electronics, among others. He is also serving as the web Editor-in-Chief of the IEEE Sensors Council. Mitradip has been elected as the Member-at-Large of the IEEE Sensors Council, USA in 2025.

Authorized licensed use limited to: UNIVERSITY COLLEGE CORK. Downloaded on October 21,2026 at 10:15:57 UTC from IEEE Xplore. Restrictions apply.
© 2026 IEEE. All rights reserved, including rights for text and data mining and training of artificial intelligence and similar technologies. Personal use is permitted, but republication/redistribution requires IEEE permission. See https://www.ieee.org/publications/rights/index.html for more information.